

Free-Energy Relationships between the Proton and Hydride Donor Abilities of $[\text{HNi}(\text{diphosphine})_2]^+$ Complexes and the Half-Wave Potentials of Their Conjugate Bases

Douglas E. Berning,[†] Alex Miedaner,[†] Calvin J. Curtis,[†] Bruce C. Noll,[‡]
Mary C. Rakowski DuBois,[‡] and Daniel L. DuBois^{*,†}

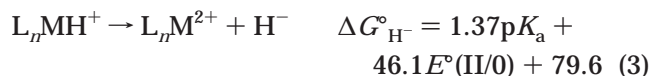
National Renewable Energy Laboratory, 1617 Cole Boulevard, Golden, Colorado,
and Department of Chemistry and Biochemistry, University of Colorado, Boulder, Colorado

Received January 24, 2001

A linear free-energy relationship exists between the half-wave potentials of the (II/I) couples of $\text{Ni}(\text{diphosphine})_2$ complexes and the hydride donor ability ($\Delta G^\circ_{\text{H}^-}$) of the corresponding $[\text{HNi}(\text{diphosphine})_2]^+$ complexes. A similar correlation is observed between the half-wave potentials of the (I/0) couples of $\text{Ni}(\text{diphosphine})_2$ complexes and the $\text{p}K_{\text{a}}$ values (or $\Delta G^\circ_{\text{H}^+}$) of the corresponding $[\text{HNi}(\text{diphosphine})_2]^+$ complexes. As a result, it is possible to use the potentials of these two couples to predict the free energies of all three Ni–H bond cleavage reactions, $\Delta G^\circ_{\text{H}^+}$, $\Delta G^\circ_{\text{H}^\bullet}$, and $\Delta G^\circ_{\text{H}^-}$, for this class of nickel complexes. The molecular structures of $\text{Ni}(\text{Et}_2\text{PCH}_2\text{CH}_2\text{PPh}_2)_2$ and $\text{Ni}(\text{Ph}_2\text{PCHCHPPh}_2)_2$ were determined by single-crystal X-ray diffraction studies.

Introduction

Transition metal hydride complexes are important intermediates in a number of catalytic reactions, and a better understanding of the factors controlling the thermodynamic properties of the M–H bond would be useful in designing catalytic reactions. The M–H bond can be cleaved in three ways, as shown in reactions 1–3.



The free energy of deprotonation, reaction 1, is generally obtained by measuring the equilibrium constant for a proton transfer reaction between the metal hydride and a base whose $\text{p}K_{\text{a}}$ value is known.¹ The energetics for the homolytic cleavage of the M–H bond, reaction 2, have been measured by several techniques.² One of the easiest is based on a thermodynamic cycle that uses $\text{p}K_{\text{a}}$

values of metal hydride complexes and the one-electron oxidation potentials of the conjugate bases of the hydrides.^{3–7} The constants (kcal/mol) shown in eqs 2 and 3 are appropriate when acetonitrile is used as a solvent and the potentials are referenced to the ferrocene/ferrocenium couple taken as 0 V. Recently, free-energy measurements for reaction 3 have been reported. One study was based on hydride transfer reactions from organic reagents of known hydride donor ability.⁸ The other was based on a thermodynamic cycle that uses the $\text{p}K_{\text{a}}$ values of the hydrides and the two-electron oxidation potentials of the conjugate bases of the hydrides to calculate the free energy of hydride transfer, as shown in eq 3.⁹

For many metal hydrides, it is not possible to obtain reversible electrochemical data for the conjugate base because rapid dimerization reactions occur following oxidation.^{3–7} The complexes formed on deprotonation of the $\text{HM}(\text{diphosphine})_2$ and $[\text{HM}(\text{diphosphine})_2]^+$ complexes of the cobalt and nickel triads are unusual in that they generally undergo two reversible one-electron

[†] National Renewable Energy Laboratory.

[‡] University of Colorado.

(1) (a) Kristjánssdóttir, S. S.; Norton, J. R. In *Transition Metal Hydrides: Recent Advances in Theory and Experiment*; Dedieu, A., Ed.; VCH: New York, 1991; pp 309–359. (b) Jordan, R. F.; Norton, J. R. *J. Am. Chem. Soc.* **1982**, *104*, 1255–1263. (c) Moore, E. J.; Sullivan, J. M.; Norton, J. R. *J. Am. Chem. Soc.* **1986**, *108*, 2257–2263. (d) Kristjánssdóttir, S. S.; Moody, A. E.; Weberg, R. T.; Norton, J. R. *Organometallics* **1988**, *7*, 1983–1987. (e) Jessop, P. G.; Morris, R. H. *Coord. Chem. Rev.* **1992**, *121*, 155. (f) Bullock, R. M.; Song, J.-S.; Szalda, D. J. *Organometallics* **1996**, *15*, 2504–2516. (g) Davies, S. C.; Henderson, R. A.; Hughes, D. L.; Oglieve, K. E. *J. Chem. Soc., Dalton Trans.* **1998**, 425–431. (h) Abdur-Rashid, K.; Fong, T. P.; Greaves, B.; Gusev, D. G.; Hinman, J. G.; Landau, S. E.; Lough, A. J.; Morris, R. H. *J. Am. Chem. Soc.* **2000**, *122*, 9155–9171.

(2) (a) Simões, J. A. M.; Beauchamp, J. L. *Chem. Rev.* **1990**, *90*, 629–688. (b) Kiss, G.; Zhang, K.; Mukerjee, S. L.; Hoff, C. D. *J. Am. Chem. Soc.* **1990**, *112*, 5657–5658. (c) Schock, L. E.; Marks, T. J. *J. Am. Chem. Soc.* **1988**, *110*, 7701–7715. (d) Wei, M.; Wayland, B. B. *Organometallics* **1996**, *15*, 4681–4683.

(3) Tilset, M.; Parker, V. D. *J. Am. Chem. Soc.* **1989**, *111*, 6711–6717; (b) **1990**, *112*, 2843.

(4) Parker, V. D.; Handoo, K. L.; Roness, F.; Tilset, M. *J. Am. Chem. Soc.* **1991**, *113*, 7493–7498.

(5) Ryan, B. O.; Tilset, M.; Parker, V. D. *J. Am. Chem. Soc.* **1990**, *112*, 2618–2626.

(6) Wayne, D. D. M.; Parker, V. D. *Acc. Chem. Res.* **1993**, *26*, 287–294.

(7) Wang, D.; Angelici, R. J. *J. Am. Chem. Soc.* **1996**, *118*, 935–942.

(8) (a) Sarker, N.; Bruno, J. W. *J. Am. Chem. Soc.* **1999**, *121*, 2174–2180. (b) Sarker, N.; Bruno, J. W. *Organometallics* **2001**, *20*, 55–61.

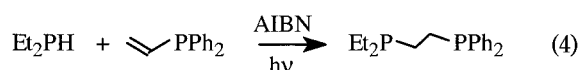
(9) Berning, D. E.; Noll, B. C.; DuBois, D. L. *J. Am. Chem. Soc.* **1999**, *121*, 11432–11447.

oxidations or a single reversible two-electron oxidation.^{9–11} If two reversible one-electron oxidations of the deprotonated metal hydride are observed and one of the three bond-cleavage reactions, 1–3, can be measured, then the free energy for all three reactions can be determined. For those complexes undergoing reversible two-electron processes, measurement of the pK_a values allows the hydride transfer potentials to be calculated, but free energies for the homolytic bond dissociation reaction cannot be obtained. Because the Ni(diphosphine)₂ complexes formed on deprotonation of the [HNi(diphosphine)₂]⁺ complexes undergo two reversible one-electron oxidation reactions, they represent an ideal opportunity for studying how various electronic and steric parameters influence all three bond-cleavage reactions, 1–3.

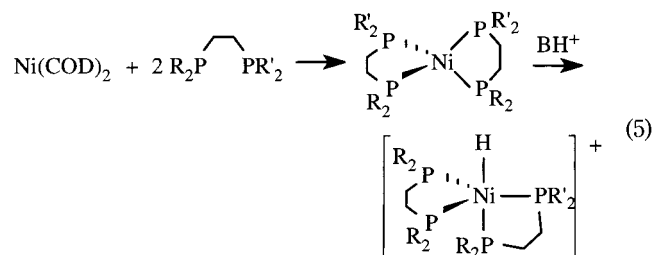
In this publication, we demonstrate that a linear free-energy correlation exists between the Ni(II/I) half-wave potentials for Ni(diphosphine)₂ complexes and the free energy associated with hydride transfer reactions of [HNi(diphosphine)₂]⁺ complexes. A similar free-energy relationship exists between the Ni(I/0) half-wave potentials and the pK_a values of the Ni–H complexes.

Results

Syntheses and Spectral Characterization of Ligands and Metal Complexes. A new ligand, Et₂-PCH₂CH₂PPh₂ (dedpe), was prepared using the free-radical addition of diethylphosphine to vinyl diphenylphosphine, reaction 4.



This free-radical reaction is a common method used for the synthesis of bidentate phosphine ligands.¹² The ³¹P NMR spectrum of dedpe consists of two doublets arising from the coupling of the two different phosphorus atoms. The coupling constants and chemical shifts are in the range expected (see Experimental Section).¹³ Reaction of Ni(COD)₂ with dedpe produces Ni(dedpe)₂ (step 1 of reaction 5).

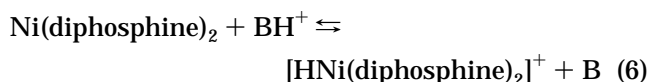


This complex exhibits an AA'XX' ³¹P NMR spectrum, as expected. Ni(dppv)₂ [where dppv is bis(diphenylphosphino)ethylene] was prepared in a similar manner and

has been reported previously.¹⁴ Spectral data are provided in the Experimental Section. Both complexes were characterized by X-ray diffraction studies, as discussed below.

Protonation of Ni(dppv)₂ and Ni(dedpe)₂ with *p*-bromoaniline·HBF₄ and anisidine·HBF₄, respectively, results in formation of the corresponding Ni–H complexes (step 2 of reaction 5). The formation of the hydride species is confirmed by their distinctive hydride resonances in the ¹H NMR spectrum. For [HNi(dedpe)₂]⁺, a triplet of triplets is observed at –13.1 ppm in the ¹H NMR spectrum. This pattern arises from coupling of the hydride ligand to two sets of two equivalent phosphorus atoms. The structure of this complex is likely a trigonal bipyramid, with an apical hydride ligand similar to those observed for HCo(dppp)₂ and HCo(dppe)₂ (where dppp is bis(diphenylphosphino)propane and dppe is bis(diphenylphosphino)ethane).^{15,16} The equivalence of the two phosphorus nuclei of the diethylphosphino groups and the two phosphorus nuclei of the diphenylphosphino groups is attributed to an exchange process. In an attempt to slow the exchange, low-temperature ³¹P NMR and ¹H NMR spectra were collected in acetone down to –90 °C. The high-temperature spectra broadened at the lowest temperature, but no low-temperature limiting spectra were observed. An IR band assigned to the Ni–H stretching mode is observed at 1934 cm^{–1}. The hydride resonance of [HNi(dppv)₂]⁺ is a quintet at –11.9 ppm. This complex is also thought to be a distorted trigonal bipyramid, and the apparent equivalence of the phosphorus atoms indicated by the ³¹P and ¹H NMR spectra is also attributed to a fluxional process.

pK_a Measurements. The pK_a values of [HNi(diphosphine)₂]⁺ complexes can be obtained by measuring equilibrium constants for the reaction of the hydrides with bases whose pK_a values are known in acetonitrile or its reverse, reaction 6.^{1,9} The pK_a value of the hydride is the sum of the pK_a value of the protonated base and pK_{eq} . In the current study, triethylamine ($pK_{BH^+} = 18.5$)¹⁷ was reacted with [HNi(dedpe)₂]⁺ to form equilibrium mixtures of the Ni(0) and Ni–H complexes. Similarly, Ni(dppv)₂ was dissolved in acetonitrile and benzonitrile solutions containing different ratios of anisidine and protonated anisidine ($pK_{BH^+} = 11.3$).^{1c} Constant ratios of the metal complexes were observed after approximately 30 min at room temperature (21 °C). Integrations of the ¹H and ³¹P NMR spectra were used to determine the equilibrium constants.



diphosphine	B	K_{eq}	solvent	pK_a
dppv	anisidine	87	acetonitrile	13.2 ± 0.2
		75	benzonitrile	13.1 ± 0.2
dedpe	NEt ₃	0.016	benzonitrile	20.3 ± 0.2

(14) Proft, B.; Porschke, K.-R. *Z. Naturforsch.* **1993**, *48b*, 919–927.

(15) Holah, D. G.; Hughes, A. N.; Maciaszek, S.; Magnuson, V. R.; Parker, K. O. *Inorg. Chem.* **1985**, *24*, 3956–3962.

(16) Ciancanelli, R.; Rakowski DuBois, M. C.; DuBois, D. L. Unpublished results.

(17) Kolthoff, I. M.; Chantooni, M. K., Jr.; Bhowmik, S. *J. Am. Chem. Soc.* **1968**, *90*, 23–28.

(10) Miedaner, A.; Haltiwanger, R. C.; DuBois, D. L. *Inorg. Chem.* **1991**, *30*, 417–427.

(11) (a) Pilloni, G.; Zotti, K. G.; Martelli, M. *J. Electroanal. Chem.* **1974**, *50*, 295–297. (b) Pilloni, G.; Vecchi, E.; Martelli, M. *J. Electroanal. Chem.* **1973**, *45*, 483–487. (c) Longato, B.; Riello, L.; Bandoli, G.; Pilloni, G. *Inorg. Chem.* **1999**, *38*, 2818–2823.

(12) (a) Uriarte, R.; Mazanec, T. J.; Tau, K. D.; Meek, D. W. *Inorg. Chem.* **1980**, *19*, 79. (b) DuBois, D. L.; Meyers, W. H.; Meek, D. W. *J. Chem. Soc., Dalton Trans.* **1975**, 1011–1015. (c) Heitkamp, S.; Lebbe, T.; Spiegel, G. U.; Stelzer, O. *Z. Naturforsch.* **1987**, *42b*, 177.

(13) Garrou, P. E. *Chem. Rev.* **1981**, *81*, 229.

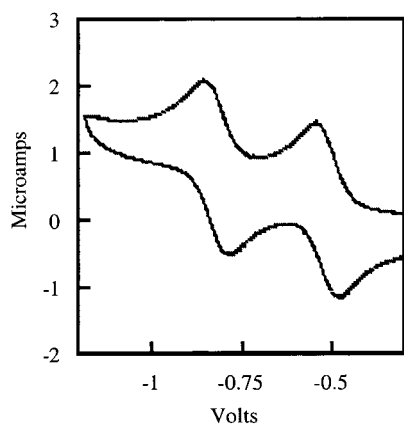


Figure 1. Cyclic voltammogram of $[\text{Ni}(\text{dppv})_2](\text{BF}_4)_2$ in a 0.3 N NEt_4BF_4 acetonitrile solution. The scan rate was 0.05 V/s, the working electrode was glassy carbon, and the potentials are given in volts vs the ferrocene/ferrocenium couple. Cathodic current is up, and anodic current is down.

pK_a values of 13.1 ± 0.2 and 13.2 ± 0.2 were determined for $\text{Ni}(\text{dppv})_2$ in benzonitrile and deuteroacetonitrile, respectively. Each value represents five different measurements. Similarly, a pK_a value of 20.3 ± 0.2 was determined for $\text{Ni}(\text{dedpe})_2$ in benzonitrile. As discussed in a preceding publication, benzonitrile has an advantage over acetonitrile for these complexes because of the higher solubility of the $\text{Ni}(0)$ complexes in benzonitrile compared to acetonitrile.⁹

Electrochemical Measurements. A cyclic voltammogram of $[\text{Ni}(\text{dppv})_2](\text{BF}_4)_2$ in acetonitrile is shown in Figure 1. It consists of two reversible one-electron reductions at -0.52 and -0.83 V vs the ferrocene/ferrocenium couple. The peak-to-peak separations of the $\text{Ni}(\text{II/I})$ and $\text{Ni}(\text{I/0})$ couples are 65 and 67 mV, respectively, compared to an expected value of 60 mV for a fully reversible one-electron process with no resistance effects, and the ratios of the cathodic and anodic peak heights are unity within experimental error (1.0 ± 0.1). The waves are diffusion-controlled, as indicated by a linear plot of the peak height vs the square root of the scan rate. The electrochemical behavior of $\text{Ni}(\text{dedpe})_2$ is comparable with half-wave potentials at -0.99 V (II/I) and -1.08 V (I/0) vs the ferrocene/ferrocenium couple in acetonitrile.

Structural Studies. Single crystals of $\text{Ni}(\text{dedpe})_2$ and $\text{Ni}(\text{dppv})_2$ were grown by deprotonation of the corresponding hydrides with an appropriate base in acetonitrile. Crystallographic data for these two complexes are given in Table 1. Two independent molecules are observed in the unit cell of $\text{Ni}(\text{dppv})_2$. One of these independent molecules exhibits a 10% disorder with a third molecule. Selected bond distances and angles for $\text{Ni}(\text{dedpe})_2$ and $\text{Ni}(\text{dppv})_2$ are given in Table 2. Drawings of $\text{Ni}(\text{dedpe})_2$ and $\text{Ni}(\text{dppv})_2$ are shown in Figure 2. Both complexes exhibit a distorted tetrahedral structure. The dihedral angle between the two planes formed by the Ni atom and the two phosphorus atoms of each dedpe ligand is 84.9° . The two independent molecules of $\text{Ni}(\text{dppv})_2$ have dihedral angles of 83.6° and 81.2° . The mean of the P-Ni-P bond angles of the diphosphine ligands is 90.9° for $\text{Ni}(\text{dedpe})_2$ and 90.7° for $\text{Ni}(\text{dppv})_2$, respectively. These values are significantly larger than

Table 1. Crystallographic Data for $\text{Ni}(\text{dedpe})_2$ ($\text{dedpe} = \text{Et}_2\text{PCH}_2\text{CH}_2\text{PPh}_2$) and $\text{Ni}(\text{dppv})_2$ ($\text{dppv} = \text{Ph}_2\text{PCHCHPh}_2$)

	$\text{Ni}(\text{dedpe})_2$	$\text{Ni}(\text{dppv})_2$
empirical formula	$\text{C}_{36}\text{H}_{48}\text{NiP}_4$	$\text{C}_{52}\text{H}_{44}\text{NiP}_4$
formula mass	663.33	851.46
crystal system	orthorhombic	triclinic
space group	$Pbca$	$P\bar{1}$
a , Å	18.4789(9)	11.5923(6)
b , Å	19.0693(9)	17.0717(8)
c , Å	19.6335(9)	22.9546(11)
α , deg	90	72.0620(10)
β , deg	90	81.5110(10)
γ , deg	90	83.4050(10)
volume, Å ³	6918.4(6)	4262.9(4)
Z , formula units/cell	8	4
density(calcd), $\text{Mg}\cdot\text{m}^{-3}$	1.274	1.327
abs coeff, mm^{-1}	0.769	0.641
temp, K	143(2)	143(2)
final R indices ^a	$R1 = 0.0382$, $wR2 = 0.0993$	$R1 = 0.0523$, $wR2 = 0.1273$
$[I > 2\sigma(I)]$	8281	19 110
R indices (all data)	$R1 = 0.0544$, $wR2 = 0.1096$	$R1 = 0.0742$, $wR2 = 0.1380$
goodness-of-fit ^b on F^2	1.038	1.051
largest diff peak and hole	0.614 and -0.802	2.051 and -1.498

^a $R1 = (||F_o| - |F_c||)/|F_o|$; $wR2 = \sqrt{w(F_o^2 - F_c^2)^2/w(F_o^2)^2}$. ^b $\text{GooF} = S = \sqrt{w(F_o^2 - F_c^2)^2/(M - N)}$, where M is the number of reflections and N is the number of parameters refined.

Table 2. Selected Bond Distances and Angles for $\text{Ni}(\text{dedpe})_2$ and $\text{Ni}(\text{dppv})_2$

Bond Distances (Å) for $\text{Ni}(\text{dedpe})_2$			
$\text{Ni}(1)-\text{P}(1)$	2.1407(5)	$\text{Ni}(1)-\text{P}(3)$	2.1437(5)
$\text{Ni}(1)-\text{P}(2)$	2.1527(5)	$\text{Ni}(1)-\text{P}(4)$	2.1654(5)
$\text{P}(1)-\text{C}(1)$	1.8388(17)	$\text{P}(1)-\text{C}(7)$	1.8487(17)
$\text{P}(1)-\text{C}(13)$	1.8619(17)	$\text{P}(2)-\text{C}(17)$	1.8462(18)
$\text{P}(2)-\text{C}(15)$	1.8581(18)	$\text{P}(2)-\text{C}(14)$	1.8610(17)
$\text{P}(3)-\text{C}(19)$	1.8361(18)	$\text{P}(3)-\text{C}(25)$	1.8495(17)
$\text{P}(3)-\text{C}(31)$	1.8574(17)	$\text{P}(4)-\text{C}(35)$	1.8479(18)
$\text{P}(4)-\text{C}(33)$	1.8531(17)	$\text{P}(4)-\text{C}(32)$	1.8533(19)
$\text{C}(13)-\text{C}(14)$	1.534(2)	$\text{C}(31)-\text{C}(32)$	1.533(3)
Bond Distances (Å) for $\text{Ni}(\text{dppv})_2$			
$\text{Ni}(1)-\text{P}(1)$	2.1414(6)	$\text{Ni}(1)-\text{P}(3)$	2.1484(6)
$\text{Ni}(1)-\text{P}(2)$	2.1586(6)	$\text{Ni}(1)-\text{P}(4)$	2.1594(6)
$\text{P}(1)-\text{C}(1)$	1.836(2)	$\text{P}(1)-\text{C}(13)$	1.842(2)
$\text{P}(1)-\text{C}(7)$	1.850(2)	$\text{P}(2)-\text{C}(21)$	1.832(2)
$\text{P}(2)-\text{C}(14)$	1.834(2)	$\text{P}(2)-\text{C}(15)$	1.852(2)
$\text{P}(3)-\text{C}(27)$	1.833(2)	$\text{P}(3)-\text{C}(39)$	1.838(2)
$\text{P}(3)-\text{C}(33)$	1.851(2)	$\text{P}(4)-\text{C}(40)$	1.835(2)
$\text{P}(4)-\text{C}(41)$	1.836(2)	$\text{P}(4)-\text{C}(47)$	1.850(2)
$\text{C}(13)-\text{C}(14)$	1.334(3)	$\text{C}(39)-\text{C}(40)$	1.331(3)
Bond Angles (deg) for $\text{Ni}(\text{dedpe})_2$			
$\text{P}(1)-\text{Ni}(1)-\text{P}(3)$	117.645(19)	$\text{P}(1)-\text{Ni}(1)-\text{P}(2)$	91.297(17)
$\text{P}(3)-\text{Ni}(1)-\text{P}(2)$	116.976(18)	$\text{P}(1)-\text{Ni}(1)-\text{P}(4)$	115.375(18)
$\text{P}(3)-\text{Ni}(1)-\text{P}(4)$	90.583(18)	$\text{P}(2)-\text{Ni}(1)-\text{P}(4)$	127.538(19)
$\text{C}(13)-\text{P}(1)-\text{Ni}(1)$	106.49(5)	$\text{C}(31)-\text{P}(3)-\text{Ni}(1)$	106.51(6)
$\text{C}(14)-\text{P}(2)-\text{Ni}(1)$	106.81(6)	$\text{C}(32)-\text{P}(4)-\text{Ni}(1)$	105.79(6)
$\text{C}(13)-\text{C}(14)-\text{P}(2)$	110.11(11)	$\text{C}(31)-\text{C}(32)-\text{P}(4)$	108.33(12)
$\text{C}(14)-\text{C}(13)-\text{P}(1)$	108.96(11)	$\text{C}(32)-\text{C}(31)-\text{P}(3)$	107.80(12)
Bond Angles (deg) for $\text{Ni}(\text{dppv})_2$			
$\text{P}(1)-\text{Ni}(1)-\text{P}(3)$	131.83(2)	$\text{P}(1)-\text{Ni}(1)-\text{P}(2)$	90.09(2)
$\text{P}(3)-\text{Ni}(1)-\text{P}(2)$	115.65(2)	$\text{P}(1)-\text{Ni}(1)-\text{P}(4)$	114.43(2)
$\text{P}(3)-\text{Ni}(1)-\text{P}(4)$	91.05(2)	$\text{P}(2)-\text{Ni}(1)-\text{P}(4)$	115.85(2)
$\text{C}(13)-\text{P}(1)-\text{Ni}(1)$	105.13(8)	$\text{C}(39)-\text{P}(3)-\text{Ni}(1)$	106.11(7)
$\text{C}(14)-\text{P}(2)-\text{Ni}(1)$	105.22(7)	$\text{C}(40)-\text{P}(4)-\text{Ni}(1)$	106.17(7)
$\text{C}(13)-\text{C}(14)-\text{P}(2)$	117.22(17)	$\text{C}(39)-\text{C}(40)-\text{P}(4)$	118.08(17)
$\text{C}(14)-\text{C}(13)-\text{P}(1)$	118.18(17)	$\text{C}(40)-\text{C}(39)-\text{P}(3)$	118.59(17)

P-Ni-P bond angles ($85-86^\circ$) observed for $[\text{Ni}(\text{diphosphine})_2]^{2+}$ complexes with similar ligands, indicating that these ligands accommodate changes in bite sizes

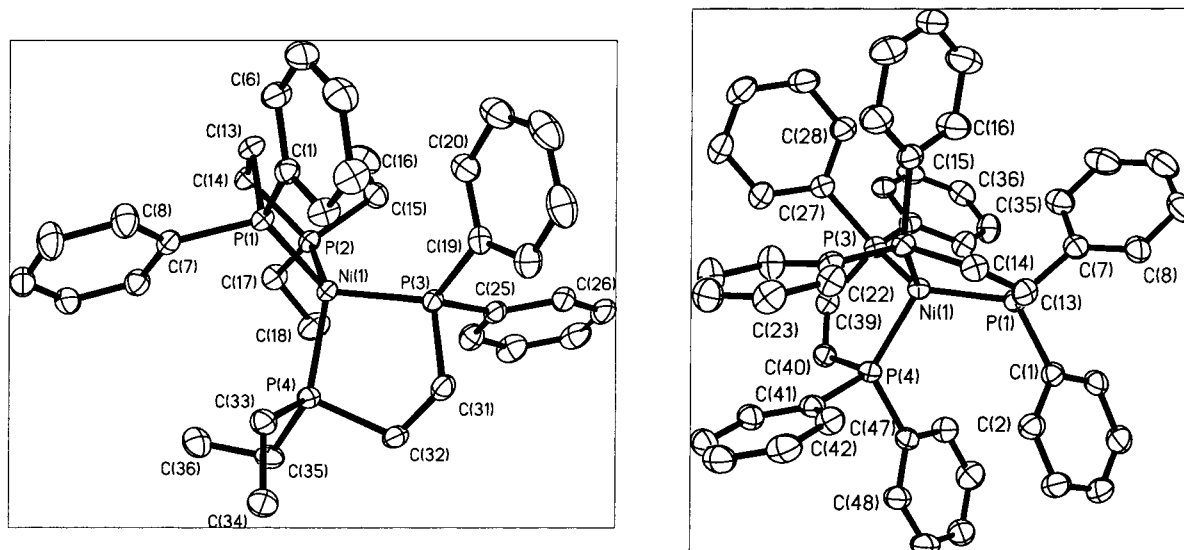


Figure 2. Drawings of Ni(dedpe)₂ and Ni(dppv)₂ showing the atom-numbering schemes.

Table 3. Thermodynamic Properties of [HNi(diphosphine)₂]⁺ Complexes (kcal/mol) and Half-Wave Potentials (V vs ferrocene) of Ni(diphosphine)₂/[Ni(diphosphine)₂]²⁺ Complexes in Acetonitrile

L ^a	E _{1/2} (II/I)	E _{1/2} (I/0)	pK _a (eq 7) ^b	ΔG° _H ⁺ (eqs 2&7, 8&9) ^b	ΔG° _H ⁺ (eq 8) ^b	pK _{BH} ⁺ ^c
dppv	−0.52	−0.83	13.2 (13.6)	52.6 (53.2, 52.9)	66.4 (66.9)	7.0
dppe ^d	−0.70	−0.88	14.2 (14.6)	52.8 (53.4, 53.8)	62.7 (63.7)	9.7
dmpp ^d	−0.89	−1.33	23.9 (24.0)	55.6 (55.8, 54.9)	61.2 (60.4)	10.8
dedpe	−0.99	−1.08	20.2 (18.8)	56.4 (54.5, 55.5)	59.8 (58.7)	11.8
depe ^d	−1.16	−1.29	23.8 (23.2)	56.5 (55.6, 56.4)	56.0 (55.7)	14.6
dmpe ^d	−1.35	−1.35	24.3 (25.3)	55.8 (57.1, 57.6)	50.7 (51.6)	18.5

^a Ligand abbreviations: dppv = Ph₂PCHCHPPh₂, dppe = Ph₂PCH₂CH₂PPh₂, dmpp = Me₂PCH₂CH₂CH₂PMe₂, dedpe = Et₂PCH₂CH₂PPh₂, depe = Et₂PCH₂CH₂PET₂, and dmpe = Me₂PCH₂CH₂PMe₂. ^b Data not in parentheses represent experimentally measured values, and data in parentheses represent values calculated from the observed half-wave potentials and the indicated equations. ^c Calculated using eq 14. ^d Electrochemical data and ΔG°_H⁺ taken from ref 9.

equally well.^{9,10,18} The nearly identical P–Ni–P bite angles for the ethylene and vinyl bridges suggest that differences in half-wave potentials observed for the Ni(dppe)₂ and Ni(dppv)₂ complexes (Table 3) are caused by differences in the electron-donating ability of the ligand bridge and not by differences in the chelate bites of these two ligands.^{9,10}

The average Ni–P bond distance in both complexes is 2.15 Å. This value is 0.06 Å shorter on average than the values found for analogous Ni(II) complexes with square-planar, tetrahedrally distorted square-planar, trigonal-bipyramidal, and square-pyramidal geometries. Although the orbital overlaps, steric interactions, and geometries are all different for these complexes, the Ni–P bond distances all fall within the range 2.21–2.23 Å.^{9,10,18} The shortening of the Ni–P bond lengths on reduction from Ni(II) to Ni(0) is also accompanied by a small increase (0.02 Å or more) in the average P–C bond lengths of the diphosphine ligands. The contraction of the Ni–P bond distances and the lengthening of the P–C bond distances are consistent with increased back-bonding to the diphosphine ligands in the Ni(0) complexes compared to the Ni(II) complexes.¹⁹

Discussion

In previous studies of [HNi(diphosphine)₂](BF₄) and [HPT(diphosphine)₂](PF₆) complexes, the diphosphine ligands dmpe, depe, dppe, and dmpp were chosen to provide information on the effects of substituents and chelate bite sizes on the thermodynamic properties of these hydrides.⁹ It was found that the hydride donor ability of these complexes is greatest for ligands with electron-donating substituents and a small chelate bite. Platinum complexes were also found to be better hydride donors than the corresponding nickel complexes. The pK_a values of these nickel and platinum hydrides depend on the electron-donating ability of the substituents and on the metal, but not on the chelate bite size of the ligand. On the basis of the limited data available for the nickel hydride complexes, it appeared that pK_a values correlated best with the Ni(I/0) couple, but three of the Ni(I/0) potentials were very similar, which prevented drawing firm conclusions. The hydricity of the nickel hydride complexes paralleled the Ni(II/I) potentials, but again, these preliminary observations were based on only four data points. In this study, we have attempted to extend this data set by carefully selecting two metal complexes for further study. The previously synthesized complex, Ni(dppv)₂, was chosen because its (II/I) (−0.52 V) and (I/0) (−0.83 V) couples are more positive than those of Ni(dppe)₂ (−0.70 and −0.88 V, respectively).^{10,14} Similarly, the (I/0) couple of Ni(dedpe)₂ should lie between those of Ni(dppe)₂ (−0.89 V) and the three basic Ni(0) complexes, Ni(dmpe)₂ (−1.39 V), Ni-

(18) (a) Alyea, C. E.; Meek, D. W. *Inorg. Chem.* **1972**, *11*, 1029. (b) Mari, A.; Gleizes, A.; Dartiguenave, M.; Dartiguenave, Y. *Inorg. Chim. Acta* **1981**, *52*, 83–85. (c) Pörschke, K.; Mynott, R.; Krüger, C.; Romão, M. J. *Z. Naturforsch.* **1984**, *39b*, 1076–1081. (d) Pörschke, K.; Mynott, R.; Angermund, K.; Krüger, C. *Z. Naturforsch.* **1985**, *40b*, 199–209. (19) (a) Woska, D.; Prock, A.; Giering, W. P. *Organometallics* **2000**, *19*, 4629–4638. (b) Landis, C. R.; Feldgus, S.; Uddin, J.; Wozniak, C. E. *Organometallics* **2000**, *19*, 4678–4886.

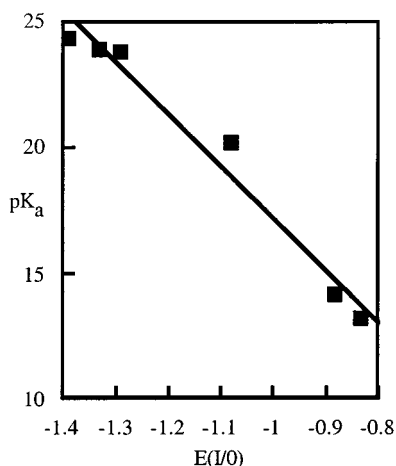


Figure 3. Plot of pK_a values for $[HNi(diphosphine)_2]X$ ($X = BF_4$ or PF_6) complexes in acetonitrile vs the potentials of the $E(I/O)$ couples of the corresponding $[Ni(diphosphine)_2](BF_4)_2$ complexes in acetonitrile.

(depe)₂ (−1.29 V), and $Ni(dmpp)_2$ (−1.33 V), which have very similar (I/O) potentials, as indicated.⁹ The value of −1.08 V found for the (I/O) couple of $Ni(dedpe)_2$ is nearly the average of the (I/O) values of $Ni(depe)_2$ and $Ni(dppe)_2$, as expected.

Table 3 lists the half-wave potentials of the (II/I) and (I/O) couples for a number of $[Ni(diphosphine)_2]^{2+}$ or $Ni(diphosphine)_2$ complexes in acetonitrile vs ferrocene. Measured pK_a values for these complexes are also shown with the free energies calculated for reactions 2 and 3 from pK_a data and redox potentials. A plot of the pK_a values vs the potentials of the (I/O) couples is shown in Figure 3. It can be seen from Figure 3 that the pK_a values exhibit a linear dependence on the (I/O) couple, with the best-fit line given by eq 7.

$$pK_a = -20.8E_{1/2}(I/O) - 3.6 \quad (7)$$

This result is similar to those of Angelici and co-workers, who demonstrated a linear correlation between the heat of protonation and the oxidation potentials of several series of complexes.⁷ To a first approximation, the potential of the (I/O) couple is a measure of the energy of the highest occupied molecular orbital of the $Ni(diphosphine)_2$ complexes, and it is reasonable that this energy would correlate well with the basicity of these complexes. Although the correlation shown in Figure 3 is not perfect ($r = 0.986$), it appears that an accurate measurement of the potentials of the (I/O) couples for $Ni(diphosphine)_2$ or $[Ni(diphosphine)_2]^{2+}$ complexes should enable the pK_a values for the corresponding $[HNi(diphosphine)_2]^+$ complexes to be predicted within approximately 1 pK_a unit.

Figure 4 shows a linear correlation for $\Delta G_{H^-}^\circ$ vs the potential of the (II/I) couple. The best-fit line is given by eq 8 ($r = 0.988$).

$$\Delta G_{H^-}^\circ = 17.5E_{1/2}(II/O) + 76.0 \quad (8)$$

This represents the first correlation of the hydricity of metal complexes with redox potentials. The potential of this couple can be interpreted as a measure of the energy of the lowest unoccupied molecular orbital (LUMO) of the $[Ni(diphosphine)_2]^{2+}$ complexes, which

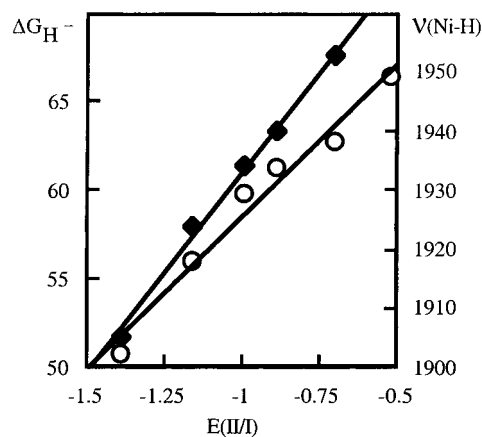


Figure 4. Plots of $\Delta G_{H^-}^\circ$ (open circles) and $\nu(Ni-H)$ (solid diamonds) for $[HNi(diphosphine)_2]X$ ($X = BF_4$ or PF_6) vs the potential of the $E(II/I)$ couples for the corresponding $[Ni(diphosphine)_2](BF_4)_2$ complexes in acetonitrile.

is the antibonding $d_{x^2-y^2}$ orbital. As this is the acceptor orbital for hydride ligands in hydride transfer reactions, it is also reasonable that the energy of this orbital would correlate with the hydride acceptor ability of the $[Ni(diphosphine)_2]^{2+}$ complexes. The energy of this orbital is affected by the electron donor ability of the substituents on the diphosphine ligands and by a tetrahedral distortion of these square-planar complexes. As the substituents on the phosphorus atoms become more electron donating, the energy of the LUMO increases. That is, the potentials of the (II/I) couple become more negative, and this leads to poorer hydride acceptors or better hydride donors. The energy of the $d_{x^2-y^2}$ orbital also becomes more positive (lower) as the Ni complexes undergo a tetrahedral distortion. This distortion is observed for $[Ni(dmpp)_2]^{2+}$ and $[Pt(dmpp)_2]^{2+}$, and it decreases the antibonding interaction between the σ orbital of the phosphorus atoms and the metal $d_{x^2-y^2}$ orbital. As a result, these complexes are better hydride acceptors than might be expected based only on a consideration of the electron-donating ability of the methyl substituents. A more extensive treatment of the relationship between this distortion and molecular orbital energies has been presented previously.^{9,10}

Typically M–H stretching frequencies have been interpreted in terms of M–H bond strengths, the homolytic cleavage of the M–H bond.²⁰ However, ionic cleavage of the M–H bond may also serve as a measure of bond strength, particularly if the M–H bond is strongly polarized. As can be seen from Table 3, $\Delta G_{H^-}^\circ$ varies by less than 4 kcal/mol for the Ni complexes, while $\Delta G_{H^-}^\circ$ varies by nearly 18 kcal/mol and the pK_a values by 11.1 units (15 kcal/mol). These data suggest that it is the ionic component of the Ni–H bond that varies the most in this series of complexes. If the Ni–H bond is polarized with negative charge on the hydrogen atom and positive charge on nickel, then the Ni–H stretching frequencies may be more closely related to the hydride transfer reaction than to the homolytic bond dissociation energy. The heterolytic cleavage of the

(20) (a) Pleune, B.; Morales, D.; Meunier-Prest, R.; Richard, P.; Collange, E.; Fetting, J. C.; Poli, R. *J. Am. Chem. Soc.* **1999**, *121*, 2209–2225. (b) For Si–H bonds: Chatgililoglu, C.; Guerrini, A.; Lucarini, M. *J. Org. Chem.* **1992**, *57*, 3405–3409. (c) For C–H bonds: McKean, D. C. *Int. J. Chem. Kinet.* **1989**, *21*, 445.

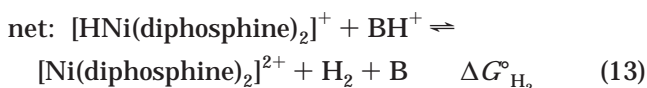
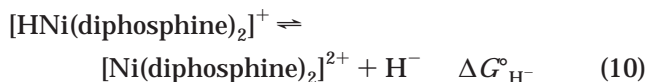
Ni–H bond can be regarded as a very long hydride stretch; that is, the positive and negative charges are effectively moved to infinity. For strongly acidic metal hydrides, the M–H bond strength may correlate with the acidity or pK_a values of the metal hydrides, because the M–H bond may be polarized in the M^+H^- direction. For the Ni complexes studied in this work the correlation of the Ni–H stretching frequency with the Ni(I/0) couple is poor ($r = 0.78$). This is the redox couple that shows a strong correlation with the pK_a values. Similarly, the correlation of the Ni–H stretching frequency with $\Delta G^\circ_{H^-}$ for the Ni–H bond is poor ($r = 0.57$). For these Ni complexes, the Ni–H stretching frequencies correlate best with the (II/I) couples of the Ni(diphosphine)₂ complexes ($r = 0.998$) or the hydride donor abilities of the $[HNi(diphosphine)_2]^+$ complexes.

Using the plot in Figure 3 or eq 7 and the potentials of the (I/0) couples, the pK_a values of the corresponding $[HNi(diphosphine)_2]^+$ complexes can be predicted with reasonable accuracy. This is seen by a comparison of the pK_a values calculated using eq 7 (shown in parentheses in Table 3) with the experimentally measured values. The agreement is typically within 1 pK_a unit. Similarly, from the plots in Figure 4 or eq 8 and the (II/I) potentials, the hydride donor abilities of the corresponding $[HNi(diphosphine)_2]^+$ complexes can be estimated ($\Delta G^\circ_{H^-}$ values shown in parentheses for Table 3). The agreement with the experimentally determined value is generally within 1.5 kcal/mol. The estimated pK_a can also be used to calculate $\Delta G^\circ_{H^-}$ for reaction 2 using the corresponding equation and a measured (I/0) potential. These values are listed in Table 3 as the first member of the ordered pair shown in parentheses following the experimental value of $\Delta G^\circ_{H^-}$. $\Delta G^\circ_{H^-}$ for reaction 2 can also be calculated from the Ni(II/I) couple, an estimated $\Delta G^\circ_{H^-}$ from eq 8, and eq 9.

$$\Delta G^\circ_{H^-} = \Delta G^\circ_{H^-} - 23.06E_{1/2}(II/I) - 26.0 \quad (9)$$

These values are shown as the second member of the ordered pair shown in parentheses following the experimental value. These values are also generally within 1.5 kcal of the experimental values. These results indicate that all three free-energy values associated with the Ni–H bond can be determined with reasonable accuracy from the potentials of the (II/I) and (I/0) couples of the Ni(diphosphine)₂ complexes.

The ability to predict these thermodynamic parameters can be extremely valuable for predicting and understanding reactions of these complexes. For example, the protonation of Ni(diphosphine)₂ complexes can lead to the formation of $[HNi(diphosphine)_2]^+$ complexes or to $[Ni(diphosphine)_2]^{2+}$ complexes and H₂ depending on the strength of the acid used. Plots similar to those in Figures 3 and 4 (or eqs 7 and 8) can be used to predict the pK_a range over which $[HNi(diphosphine)_2]^+$ complexes will be stable. Only acids with pK_a values lower than the pK_a values listed in Table 3 will be capable of protonating the Ni(diphosphine)₂ complexes to form a hydride. Similarly, the hydride donor abilities or $\Delta G^\circ_{H^-}$ values of $[HNi(diphosphine)_2]^+$ can be used to calculate the free energy associated with protonation of the $[HNi(diphosphine)_2]^+$ complexes to form hydrogen ($\Delta G^\circ_{H_2}$), as shown by the thermodynamic cycle given by eqs 10–13.



Reaction 10 is the hydride donor reaction, and the free energy associated with this reaction is of course $\Delta G^\circ_{H^-}$. Reaction 11 is the deprotonation of BH^+ to form B with a free energy of $1.37pK_{BH^+}$. Reaction 12 is the reverse of the heterolytic cleavage of hydrogen in acetonitrile. The ΔG° value for this reaction (-76.0 kcal/mol) can be calculated from the free energy for the homolytic cleavage of H₂ in acetonitrile (103.6 kcal/mol)⁶ and the free energies for the reduction of H⁺ (53.6 kcal/mol see reaction 2)^{6,9} and H[•] (-26.0 kcal/mol)⁶ in acetonitrile. The sum of reactions 10–12 is the protonation of a $[HNi(diphosphine)_2]^+$ complex to form hydrogen, reaction 13. The free energy of this reaction ($\Delta G^\circ_{H_2}$) is the sum of the free energies associated with reactions 10–12. If $\Delta G^\circ_{H_2}$ is set to 0, then the value of pK_{HB^+} for which reaction 13 will be at equilibrium can be calculated (eq 14).

$$pK_{BH^+} = (76.0 - \Delta G^\circ_{H^-})/1.37 \quad (14)$$

These values are shown for each complex in Table 3 (pK_{BH^+}). Acids having pK_a values less than the pK_{BH^+} values shown in Table 3 are thermodynamically capable of protonating the corresponding $[HNi(diphosphine)_2]^+$ complexes to form hydrogen. $[HNi(diphosphine)_2]^+$ complexes are expected to be thermodynamically stable to acids having pK_a values greater than the pK_{BH^+} values shown in Table 3 and to bases whose pK_{BH^+} values are less than the pK_a values shown in Table 3. For example, in Table 3 the pK_a value of $[HNi(dppv)_2]^+$ is 13.2 and the pK_{BH^+} value is 7.0. This means that protonated *p*-bromoaniline (*p*-BrC₆H₄NH₃⁺), whose pK_{BH^+} value is 9.6, should protonate Ni(dppv)₂ to form $[HNi(dppv)_2]^+$, but this hydride should not be protonated by *p*-BrC₆H₄NH₃⁺ to form hydrogen and $[Ni(dppv)_2]^{2+}$. Thus a knowledge of the potentials of the (I/0) and (II/I) couples can be used to select acids for protonating Ni(diphosphine)₂ complexes without resulting in a second protonation to form hydrogen and Ni(II). This can be useful for designing reactions to prepare the desired hydrides or for selecting reaction conditions for which the hydrides will be stable.

Summary and Conclusions

A linear free-energy relationship is shown to exist between the half-wave potentials of the (II/I) couples of Ni(diphosphine)₂ complexes and the hydride donor ability ($\Delta G^\circ_{H^-}$) of the corresponding $[HNi(diphosphine)_2]^+$ complexes. This is the first quantitative correlation of transition metal hydricities with an easily measured spectroscopic or electrochemical parameter. A similar correlation also exists between the half-wave

potentials of the (I/O) couples of Ni(diphosphine)₂ complexes and the pK_a values of the corresponding [HNi(diphosphine)₂]⁺ complexes. As a result, it is possible to use the potentials of these two couples to predict the free energies of all three Ni–H bond cleavage reactions, $\Delta G^\circ_{H^+}$, $\Delta G^\circ_{H^-}$, and $\Delta G^\circ_{H^\cdot}$, for this class of nickel complexes.

Experimental Section

Physical Measurements and General Procedures. ¹H and ³¹P NMR spectra were recorded on a Varian Unity 300 MHz spectrometer at 299.95 and 121.42 MHz, respectively. ¹H chemical shifts are reported relative to tetramethylsilane using residual solvent protons as a secondary reference. ³¹P chemical shifts are reported relative to external phosphoric acid. In experiments where accurate integrations of ³¹P resonances were required, spectra were collected using a 52° pulse and a repetition rate of 11.96 s. This is sufficient to allow complete relaxation of nuclei with $T_1 < 27$ s. Measured T_1 values for Ni(dedpe)₂ and Ni(dedpe)₂H⁺ were 1.1 and 3.5 s, respectively. Infrared spectra were recorded on a Nicolet 510P spectrometer as Nujol mulls. Elemental analyses were performed by Galbraith Laboratories, Inc., Knoxville, TN. All syntheses were carried out using Schlenk and drybox techniques.

X-ray Diffraction Studies. Crystals were manipulated under a light hydrocarbon oil. The datum crystal was affixed with a small amount of silicone stopcock grease to a thin glass fiber attached to a tapered copper mounting-pin. This assembly was transferred to the goniometer of a Bruker SMART CCD diffractometer equipped with an LT-2a low-temperature apparatus operating at 143 K.

Ni(dedpe)₂. Cell parameters were determined using reflections harvested from a series of three orthogonal sets of 20 0.3° ω scans. Final cell parameters were refined using 7820 reflections with $I > 10\sigma(I)$ chosen from the entire data set. All data were corrected for Lorentz and polarization effects, as well as for absorption.

Structure solution in centrosymmetric space group *Pbca* revealed the heavy atom positions and many of the carbon positions. Additional carbon sites were located after four cycles of least-squares refinement followed by difference Fourier synthesis. Hydrogen atoms were placed at calculated geometries and allowed to ride on the position of the parent atom. All non-hydrogen atoms were refined with anisotropic parameters for thermal motion. Thermal parameters for hydrogen atoms were set to 1.2 times the equivalent isotropic U of the parent. The final difference map was essentially flat and featureless.

Ni(dppv)₂. Cell parameters were determined using reflections harvested from a series of three orthogonal sets of 20 0.3° ω scans. Final cell parameters were refined using 6896 reflections with $I > 10\sigma(I)$ chosen from the entire data set. All data were corrected for Lorentz and polarization effects, as well as for absorption.

Solution of the structure in the centrosymmetric space group *P1* revealed two crystallographically independent molecules. Additional atoms of these molecules were located via least-squares refinement followed by difference Fourier synthesis. Hydrogen atoms were placed at calculated positions, which were allowed to ride on the position of the parent atom. Non-hydrogen atoms were refined with anisotropic parameters for thermal motion; hydrogen thermal motion was modeled at 1.2 times the equivalent isotropic U of the parent atom.

Fourier maps calculated near the final refinement indicated residual electron density near Ni(2). These 1.5 e/Å³ peaks were within bonding range for phosphorus. After adding these peaks to the model as phosphorus atoms with 0.1 site occupancy, additional peaks consistent with the ligands began to appear.

Successive Fourier maps were used to locate all carbon atoms for two more ligands. Site occupancies were refined against those of the original ligands. Final values were 0.9018(9) and 0.0982(9) for the original ligands and the new component. Neither hydrogens nor anisotropic thermal parameters were modeled for the minor component of this disorder. The angle between the normals to the planes P(7),C(91),C(92),P(8) and P(1'),C(39'),C(40'),P(2') is 96°. The disorder may be described as a 96° rotation of the molecule. After modeling this disorder, the final difference map was essentially featureless, except for a single 2.05 e/Å³ peak located 0.749 Å from Ni(2). This peak may be a result of the disorder.

Electrochemical Studies. All electrochemical experiments were carried out under an atmosphere of N₂ in 0.3 M Bu₄NBF₄ in benzonitrile or 0.3 M Et₄NBF₄ in acetonitrile. Cyclic voltammetry experiments were carried out on a Cypress Systems computer-aided electrolysis system. The working electrode was a glassy carbon disk (2 mm diameter), and the counter electrode was a glassy carbon rod. A platinum wire immersed in a permethylferrocene/permethylferrocenium solution was used as a pseudoreference electrode to fix the potential. Ferrocene was used as an internal standard, and all potentials are referenced to the ferrocene/ferrocenium couple.

Syntheses. Bis(1,5-cyclooctadiene)nickel(0), vinylidiphenylphosphine, diethylphosphine, and *cis*-1,2-bis(diphenylphosphino)ethylene were purchased from Strem Chemical Co. and used without further purification. Benzonitrile, acetonitrile, 2,2'-azobis(methylpropionitrile) (AIBN), CD₃CN, ammonium hexafluorophosphate, and triethylamine were purchased from Aldrich Chemical Co. and used as received. Anisidine was purchased from Aldrich Chemical Co. and sublimed. Tetrahydrofuran was purchased from Aldrich Chemical Co. and distilled over Na/benzophenone prior to use.

Et₂PCH₂CH₂PPh₂, dedpe. Diethylphosphine (0.62 g, 6.8 mmol), vinylidiphenylphosphine, (1.45 g, 6.8 mmol), and 2,2'-azobis(methylpropionitrile) (0.1 g) were placed in a Schlenk flask and irradiated overnight in a Rayonet photoreactor using lamps of 2537, 3000, and 3500 Å wavelengths. Volatile materials were removed in vacuo at 80 °C to produce a clear, air-sensitive oil (1.10 g, 59%). ¹H NMR (toluene-*d*₈): 7.4, 7.1, 7.0 ppm (m's, C₆H₅); 2.1, 1.4 ppm (m's, PCH₂CH₂P); 1.15 ppm (q, ³J_{HH} = 7.8 Hz, PCH₂CH₃); 0.89 ppm (dt, ³J_{PH} = 7.5 Hz, PCH₂CH₃). ³¹P NMR (toluene-*d*₈): −11.25 ppm (d, ³J_{PP} = 25 Hz, PPh₂); −17.46 ppm (d, PCH₂).

Ni(dedpe)₂. A 100 mL Schlenk flask was charged with dedpe (1.20 g, 4.42 mmol) in THF (50 mL). Ni(COD)₂ (0.60 g, 2.18 mmol) was added slowly at room temperature. The orange reaction mixture was stirred for 2 h and the solvent removed in vacuo. The yellow product was washed with acetonitrile (3 × 40 mL) and dried in vacuo (0.96 g, 72%). Anal. Calcd for C₃₆H₄₈NiP₄: C, 65.2; H, 7.3. Found: C, 64.3; H, 7.5. ¹H NMR (toluene-*d*₈): 7.0–7.8 ppm (m, PC₆H₅); 0.76 and 1.23 ppm (m, PCH₂CH₃); 2.2, 1.68, 1.42, and 1.23 ppm (m, PCH₂CH₂P and PCH₂CH₃). ³¹P NMR (toluene-*d*₈): AA'XX' spectrum; 49.3 ppm (m, $N = 80$ Hz, PPh₂); 41.7 ppm (m, PCH₂). X-ray quality crystals of Ni(dedpe)₂ were grown by using excess triethylamine to deprotonate [HNi(dedpe)₂](BF₄) in acetonitrile. Yellow crystals form slowly at room temperature over a period of several hours.

Ni(dppv)₂. This compound was prepared using a literature procedure.¹⁴ ¹H NMR (toluene-*d*₈): 6.82–7.35 (m's, Ph and ethylene protons). ³¹P NMR (toluene-*d*₈): 51.5 (s). X-ray quality crystals were obtained by protonating Ni(dppv)₂ with [*p*-C₆H₄-(OCH₃)(NH₃)]BF₄ in acetonitrile and back-titrating with *p*-C₆H₄-(OCH₃)(NH₂). Yellow crystals form slowly at room temperature over a period of several hours.

[HNi(dedpe)₂](BF₄). A 100 mL Schlenk flask was charged with Ni(dedpe)₂ (1.0 g, 1.66 mmol) in THF (50 mL). *p*-(OCH₃)-

(21) Generally the ²J_{PH} coupling is smaller than the ³J_{PH} coupling in ethyl groups attached to phosphorus (see ref 9).

$\text{C}_6\text{H}_4(\text{NH}_3)\text{BF}_4$ (0.36 g, 1.70 mmol) was added at room temperature, and the reaction mixture stirred for 30 min. The solvent was removed from the reaction mixture in vacuo, and the resulting yellow solid was washed with toluene (3×30 mL) and dried in vacuo (1.01 g, 81%). Anal. Calcd for $\text{C}_{36}\text{H}_{45}\text{P}_4\text{BF}_4\text{Ni}$: C, 57.9; H, 6.1. Found: C, 57.1; H, 6.6. ^1H NMR (acetonitrile- d_3): 7.1–7.6 ppm (m, PC_6H_5); 1.18 and 0.88 ppm (m, PCH_2CH_3); 1.4–2.4 ppm (m, $\text{PCH}_2\text{CH}_2\text{P}$ and PCH_2CH_3); –13.1 (tt, $^2J_{\text{PH}} = 25$ and 15 Hz, Ni- H). ^{31}P NMR (acetonitrile- d_3): AA'XX' spectrum; 48.6 ppm (m, PPh_2); 47.5 ppm (m, PEt_2). IR Nujol: $\nu(\text{Ni-H})$ 1934 cm^{-1} .

[HNi(dppv) $_2$](BF $_4$). This complex can be prepared from Ni(dppv) $_2$ and [p -BrC $_6$ H $_4$ (NH $_3$)]BF $_4$ in 90% yield using the procedure for [HNi(dedpe) $_2$](PF $_6$). ^1H NMR (acetonitrile- d_3): 7.08 and 7.26 ppm (m's, Ph and ethylene protons); –11.87 (quintet, $^2J_{\text{PH}} = 10$ Hz, Ni- H). ^{31}P NMR (acetonitrile- d_3): 56.71 ppm (s). No band could be unambiguously assigned to the Ni–H stretch in the IR spectrum.

pK_a of [HNi(dppv) $_2$](BF $_4$) in Benzonitrile and Acetonitrile. These experiments were performed by first preparing two solutions in a drybox. The first solution contained Ni(dppv) $_2$ (1.41×10^{-2} M) and [p -C $_6$ H $_4$ (OCH $_3$)(NH $_3$)]BF $_4$ (1.90×10^{-2} M) in benzonitrile. Full conversion to the metal hydride was determined by ^{31}P NMR spectroscopy. A second solution of p -C $_6$ H $_4$ (OCH $_3$)(NH $_2$) (1.40 M) was also prepared in benzonitrile. Various amounts of the second solution were added to 0.5 mL aliquots of the first solution followed by benzonitrile to give a constant volume of 0.75 mL. A total of five samples were prepared in this fashion. The samples were allowed to equilibrate for at least 30 min, and the relative concentrations of the species present were calculated by integration of the

^{31}P NMR signals. The same ratios were observed within experimental error from 15 min to 1 day. Similar experiments were performed in deuteroacetonitrile. The latter experiments were accompanied by the formation of red crystals of Ni(dppv) $_2$. However, sufficient Ni(dppv) $_2$ remained in solution to permit accurate integration.

pK_a of [HNi(dedpe) $_2$](PF $_6$) in Benzonitrile. This experiment was performed by preparing a 1.41×10^{-2} M solution of [Ni(dedpe) $_2$ H]PF $_6$ in benzonitrile in a drybox. Various amounts of triethylamine in benzonitrile (1.40 M) were added to 0.75 mL of the [Ni(dedpe) $_2$ H]PF $_6$ followed by benzonitrile to give a constant volume of 1.00 mL. The mixtures were equilibrated for at least 30 min, and the relative concentrations of the species present were calculated by integration of the ^{31}P NMR signals.

Acknowledgment. This work was supported by the U.S. Department of Energy, Office of Science, Chemical Sciences Division. M.C.R.D. would like to acknowledge the support of the National Science Foundation.

Supporting Information Available: Tables of crystal data, data collection parameters, structure solution and refinement, atomic coordinates and equivalent isotropic displacement parameters, bond lengths, bond angles, anisotropic thermal parameters, and hydrogen coordinates and isotropic displacement parameters for Ni(dedpe) $_2$, and Ni(dppv) $_2$. This information is available free of charge via the Internet at <http://pubs.acs.org>.

OM0100582